

A modified Allen-Cahn model for pattern synthesis on surfaces

Lorina Dascal Gautam Pai Ron Kimmel

Technion - Israel Institute of Technology
{lorina,paigautam,ron}@cs.technion.ac.il



Figure 1: Various patterns on the surface by means of modified Allen-Cahn model. Left: Inverted spots. Right: Spots.

Abstract

We propose an extension of the Allen-Cahn model for pattern synthesis on two dimensional curved surfaces. This model is based on a single PDE and it offers improved ability of controlling the type of generated surface patterns via the chosen reaction-diffusion coefficient, thus, obtaining patterns in form of spots, inverted spots, or stripes. We investigate the dependence of the type of the obtained pattern on the new proposed reaction term. An efficient operator splitting scheme is used to discretize the model on a surface. Experiments on surfaces with varying initial conditions illustrate a variety of patterns.

1 Introduction

The Allen-Cahn equation is a semilinear reaction diffusion based PDE, and has been widely used in phase separation, crystal-growth and various material science applications defined on planar domains. It was originally introduced in J.W.Cahn [1979] as a model for the motion of anti-phase boundaries in a binary alloy. It was later used in phase separation Chen [2002], or crystal growth analysis Warren [2008]. A study of a different semi-linear reaction-diffusion equation, governed by the Hamiltonian operator was proposed in Pai and Kimmel [2018], altogether with applications for 3D spectral mesh geometry compression. In this paper, we explore the behaviour of an extension of the Allen-Cahn reaction-diffusion partial differential equation on triangulated surfaces and analyze its generated patterns, which will be shown to exhibit a richer set of patterns compared to the regular Allen-Cahn equation itself. Turing models and in general reaction-diffusion systems have been extensively used for understanding spatial patterns. Patterns arising in reaction-diffusion processes have been proposed in biology applications to describe developmental processes such as skin pigmentation patterning Kondo [2011]. The solvers used in various publications involve more advanced numerical methods for solving the reaction-diffusion system, especially when applied on a curved domain. Allen-Cahn PDE was applied to two dimensional flat domain, as well as to curved surfaces, for which various numerical solvers were analyzed in Piret [2013], Elliott [2007]. However, the only pattern that can be obtained with this model is a stripe-based structure. Its complement in the large class of reaction diffusion systems is the Fitzhugh-Nagumo reaction-diffusion system, see Yoshizawa [1962], which contains in its nonlinear part a third order polynomial. It can generate patterns like spots/stripes, but at the cost of solving a nonlinear coupled PDE system. In this paper, we propose a simple extension of the Allen-Cahn model, exhibiting richer patterns on general non-flat geometries by means of a single PDE defined on the surface. We analyze the behavior of the suggested model with its newly introduced reaction term and handle it numerically by an efficient operator-splitting scheme. Numerical examples illustrate the generation of spot and stripe patterns on surfaces as a function of the reaction parameter. Understanding the nature of the patterns obtained on various curved geometries is challenging. We purpose to analyze the relationship between the given coefficients of the governing reaction-diffusion equation, the underlying geometry, and the type of the resulting pattern. Moreover, the simulated numerical solution of the modified model is compactly supported, unlike the original Allen-Cahn model. Numerical experiments illustrate this important locality property.

2 Modified Allen-Cahn equation on surfaces

We describe below the modified Allen-Cahn on surfaces. Suppose Γ is a surface in \mathbb{R}^3 , and $\partial\Gamma$ is empty. The known surface Allen-Cahn (AC) equation is as

follows:

$$u_t = \Delta_\Gamma u - \frac{1}{\epsilon^2} f(u), \quad x \in \Gamma, \quad t \in [0, T] \quad (1)$$

$$u|_{t=0} = u_0(x), \quad x \in \Gamma \quad (2)$$

where $f(u) = u^3 - u$, Δ_Γ the Laplace-Beltrami operator on Γ and ϵ is a positive constant representing the interface width.

The origin of this kind of partial differential equation resides in a more general Euler functional:

$$J_\epsilon(u) = \frac{1}{2} \int_\Gamma |\nabla u|^2 dA + \int_\Gamma \frac{F(u)}{\epsilon^2} dA, \quad (3)$$

where

$$F(u) = \frac{1}{4}(u^2 - 1)^2.$$

This functional J is nothing but the free Helmholtz functional that then leads to the known Allen-Cahn equation (1). We mention other versions of the Helmholtz functional, such as logarithmic free energy functional

$$F(u) = \frac{\Theta}{2} [(1+u) \log(1+u) + (1-u) \log(1-u)] - \frac{\Theta_c}{2} u^2,$$

where Θ, Θ_c are constants) but they are not the focus of the current research.

We propose the following modified Allen-Cahn model (4):

$$u_t = \Delta_\Gamma u - \frac{1}{\epsilon^2} f_m(u), \quad x \in \Gamma, \quad t \in [0, T] \quad (4)$$

$$u|_{t=0} = u_0(x), \quad x \in \Gamma \quad (5)$$

where

$$f_m(u) = u^3 - u + b, \quad (6)$$

with b a real constant.

Its corresponding functional is a modified Helmholtz that no longer has a double-well potential.

$$J_\epsilon^m(u) = \frac{1}{2} \int_\Gamma |\nabla u|^2 dA + \int_\Gamma \frac{F_m(u)}{\epsilon^2} dA, \quad (7)$$

where

$$F_m(u) = \frac{1}{4}(u^2 - 1)^2 + bu$$

and b is a real constant.

First we prove that this modification does not change the functional property of being decreasing in time. This means that the total energy is a Lyapunov functional for the solutions of the modified Allen-Cahn equation.

Lemma 2.1 *The energy functional J_ϵ^m in (7) is decreasing in time.*

Using Green's formula

$$\int_{\Gamma} \nabla_{\Gamma} \xi \cdot \nabla_{\Gamma} \eta dA = \int_{\partial\Gamma} \xi \nabla_{\Gamma} \eta \cdot \mu ds - \int_{\Gamma} \xi \Delta_{\Gamma} \eta dA.$$

where μ is the conormal on $\partial\Gamma$. We then have by replacing $\eta = u$ and $\xi = u_t$ in the above formula and by means of integration by parts we get:

$$\begin{aligned} \frac{dJ_{\epsilon}^m(u)}{dt} &= \int_{\Gamma} \left(\nabla_{\Gamma} u \cdot \nabla_{\Gamma} u_t + \frac{F'_m(u)}{\epsilon^2} u_t \right) dA = \\ &= \int_{\Gamma} \left(-\Delta_{\Gamma} u + \frac{F'_m(u)}{\epsilon^2} \right) u_t dA = - \int_{\Gamma} u_t^2 dA \leq 0. \end{aligned}$$

This shows the decreasing behavior of the energy functional.

2.1 One dimensional case analysis

In this section we will gain some intuition on the quality of the underlying pattern by understanding the 1D behavior. Assume for the one dimensional analysis that $\epsilon = 1$. In the case when the spatial domain is an interval, we would look for stationary solutions, i.e. $\frac{du}{dt} = 0$. Thus equation (4) becomes in 1D:

$$u''(x) + (u(x) - u^3(x)) - b = 0 \quad (8)$$

Here the potential is $F(u) = - \int f_m(u) du$. with f_m given in (6).

Equation (8) can be solved analytically for $b = 0$, see Liu [2011]. Its solution is given by $u(x) = \tanh(x)$.

For $b \neq 0$, multiplying (8) by u' :

$$u''u' - f_m(u)u' = 0. \quad (9)$$

Then

$$\frac{d}{dx} \left(\frac{1}{2} \left(\frac{du}{dx} \right)^2 + F(u) \right) = 0 \quad (10)$$

That means we can easily integrate (10) as

$$\frac{1}{2} \left(\frac{du}{dx} \right)^2 + F(u) = C$$

The solution is

$$\int_{u(a)}^{u(x)} \frac{du}{\sqrt{2(C - F(u))}} = x - a$$

If we use the exact expression of the potential $F(u)$, the solution given by:

$$\int_{u(a)}^{u(x)} \frac{du}{\sqrt{2C - 0.5(1 - u^2)^2 - 2bu}} = x - a \quad (11)$$

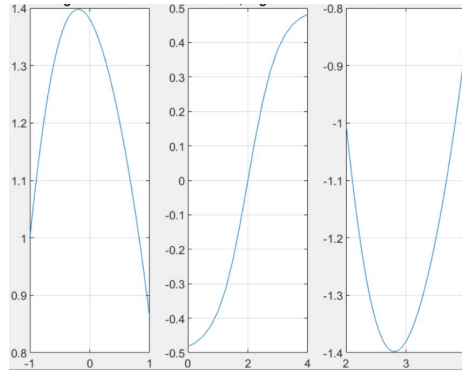


Figure 2: Left. 1D solution of modified Allen-Cahn. $b = -1$. Middle. 1D solution to Allen-Cahn. $b = 0$. Right. 1D solution of modified Allen-Cahn. $b = 1$.

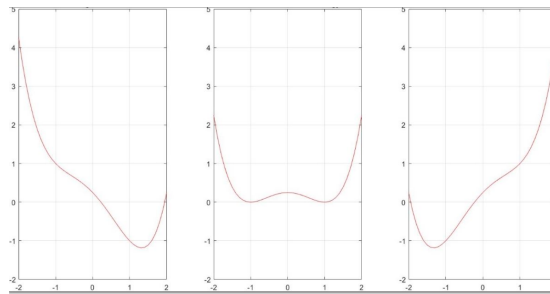


Figure 3: Modified Allen-Cahn. Energy for the various reaction coefficients. Left. $b < 0$. Middle. $b = 0$. Right $b > 0$.

We used a solver ode45 solver in Matlab to plot the numerical solution of the nonlinear ODE (for $b = 1$ and $b = -1$):

$$u'' + u(1 - u^2) - b = 0$$

Even if we cannot assert on patterns in the one dimensional case, in the graph Fig. 2 one can observe the concave up form of the solution for positive coefficient $b > 0$, as well as the concave down form of the solution for negative $b < 0$. In Fig. 3 we plotted the corresponding Lyapunov energy. As noticed in this simple one dimensional case, the solution is behaving in a clear relation with the sign of the reaction term. We will further illustrate for more complex cases of various curvy geometries, that the modified Allen-Cahn equation generates spots/ inverted spots in according to negative/positive reaction coefficients.

We further give details on the properties of the numerical scheme for discretizing the proposed model.

3 Numerical scheme

Operator splitting based scheme for modified Allen-Cahn

The splitting of the operator emerges from the structure of the polynomial structure in the reaction term that characterizes the specific structure of the AC/modified AC equation.

Denote by $\tilde{L} = L - \frac{b}{\epsilon^2}$, where L is the Laplace-Beltrami operator and by B the nonlinear part ($Bu = \frac{u-u^3}{\epsilon^2}$).

According to Strang's splitting method, the numerical solution to equation in the time interval $[t_n, t_{n+1}]$ can be written as follows:

$$U^{n+1} = (B^{\frac{\Delta t}{2}} \circ \tilde{L}^{\Delta t} \circ B^{\frac{\Delta t}{2}})U^n,$$

We will write the above splitting operator into three steps:

$$\tilde{u} = B(\tilde{u}), \tilde{u}^n = U^n, t \in [t_n, t_{n+1}] \quad (12)$$

$$\bar{u} = \Delta_\Gamma \bar{u} - \frac{b}{\epsilon^2}, \bar{u}^n = \tilde{u}^{n+1}, t \in [t_n, t_{n+1}] \quad (13)$$

$$\hat{u} = B(\hat{u}), \hat{u}^n = \bar{u}^{n+1}, t \in [t_n, t_{n+1}] \quad (14)$$

The numerical solution at $t = t_{n+1}$ is $U^{n+1} = \hat{u}^{n+1}$.

The first and third step solve the same ODE, namely a Bernoulli equation, for which one can find analytical solution.

$$\bar{u}^{n+1} = \frac{U^n}{\sqrt{e^{-\frac{2\Delta t}{\epsilon^2}} + (U^n)^2(1 - e^{-\frac{2\Delta t}{\epsilon^2}})}} \quad (15)$$

Stability of the scheme

Lemma 3.1 *For any time level $t = t_n$, the numerical solution U^n given by (15) for the first step (12) in the operator splitting is unconditionally stable.*

Proof 3.1 *We have two possible cases.*

Case A. $|U^n| \leq 1$, then

$$|\tilde{u}^{n+1}| = \frac{|U^n|}{\sqrt{(U^n)^2 + (1 - (U^n)^2)e^{-\frac{2\Delta t}{\epsilon^2}}}} \leq \frac{U^n}{\sqrt{(U^n)^2}} = 1$$

Case B. If $|U^n| > 1$, then again one has

$$|\tilde{u}^{n+1}| \leq \frac{|U^n|}{\sqrt{(1 - e^{-\frac{2\Delta t}{\epsilon^2}}) + e^{-\frac{2\Delta t}{\epsilon^2}}}} = |U^n|$$

Combining the two cases, one can show

$$\|\tilde{u}^{n+1}\|_\infty \leq \max\{\|U^n\|_\infty, 1\},$$

which completes the proof.

A similar Lemma can be formulated for the third step too.

The second step of the splitting involves discretization of the operator \tilde{L} , i.e. the Laplace Beltrami operator, for which we use cotan weight scheme for triangulated meshes. The Laplace Beltrami operator is discretized by $L = A^{-1}W$, where A is the diagonal matrix of the Voronoi cells areas around a vertex.

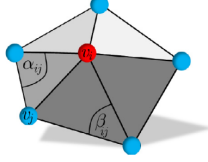


Figure 4: Weights in Discrete Laplacian

$$W_{ij} = \begin{cases} \sum_{v_j \in N_i} w_{ij}, & i = j \\ -w_{ij}, & i \neq j, v_j \in N_i \\ 0, & \text{otherwise} \end{cases}$$

and the weights $w_{ij} = \cot \alpha_{ij} + \cot \beta_{ij}$ where α_{ij} and β_{ij} are the angles opposite to the edge as appearing in Fig 4. If a small step time parameter is used, step two of the operator splitting scheme is stable.

Remark 3.1 *The operator splitting scheme (12), (13), (14) is stable only under small time-step restriction. To obtain a fully unconditionally operator splitting scheme, one might further use a full FEM or a Crank-Nicolson scheme for discretizing the part involving the Laplace-Beltrami operator.*

4 Numerical examples

4.1 Global Patterns with modified Allen-Cahn model

In this section we will show numerical experiments of phase separation as a result of applying Allen-Cahn model as well as modified A-C model on various surfaces to show the generated patterns. While with Allen-Cahn PDE, the only pattern that can be obtained is a stripe based shape, the modified new model allows generating various patterns in form of spots/inverted spots on the surfaces and an operator-splitting scheme is used to easily implement it.

The characteristics of the resulting patterns obtained by applying the modified Allen-Cahn (4) model are determined according to the values of the constant b . The following types of patterns can be generated (see Fig.5-Fig.10): for $b > 0$ inverted spots, for $b < 0$ spots, and for $b = 0$, stripes, i.e. regular Allen-Cahn. The generated pattern can be categorized, as seen in the numerical experiments on various surfaces, as follows: when $0 < b < 0.3$, one obtains inverted spots,

when $-0.3 < b < 0$ one gets spots, while for values $|b| > 0.3$, the diffusion term takes over the reaction one, and one gets a trivial constant solution as time progresses.

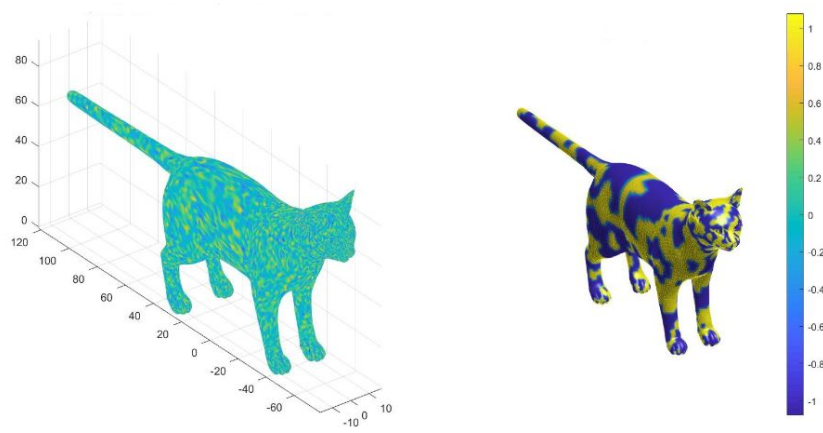


Figure 5: Allen-Cahn on an animal surface. Left: Random initial data. Right: Stripes by Allen-Cahn. Reaction term: $b = 0$.

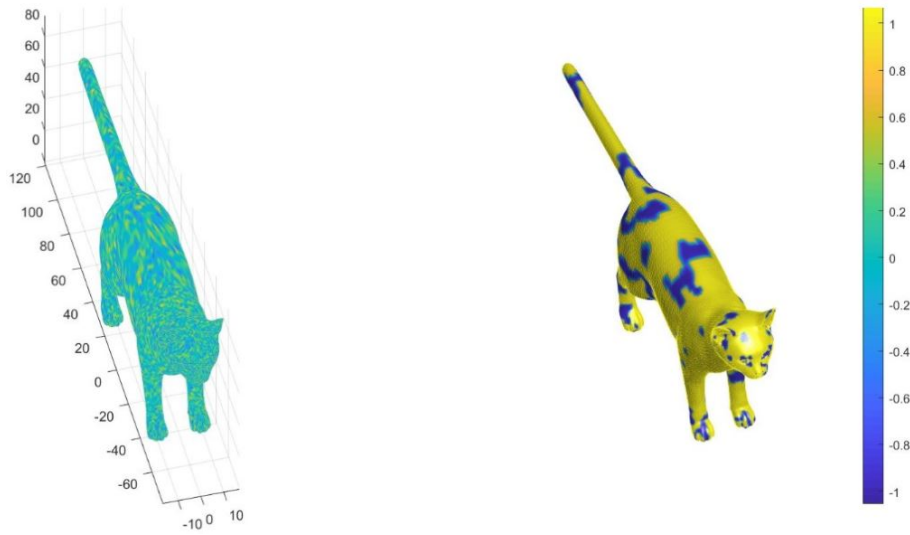


Figure 6: Left: Random initial data. Right: Inverted spots. Reaction term : $b = 0.2$.

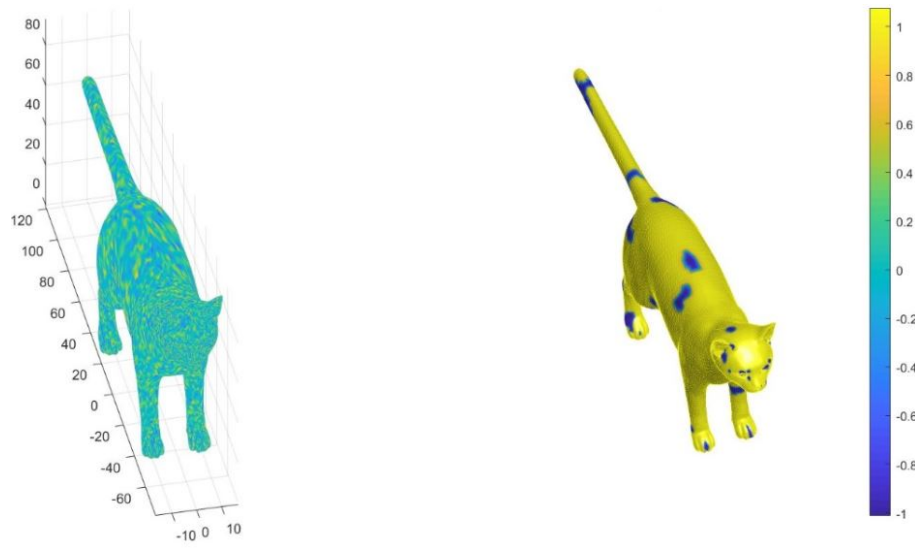


Figure 7: Left: Random initial data. Right: Inverted spots. Reaction term : $b = 0.3$.

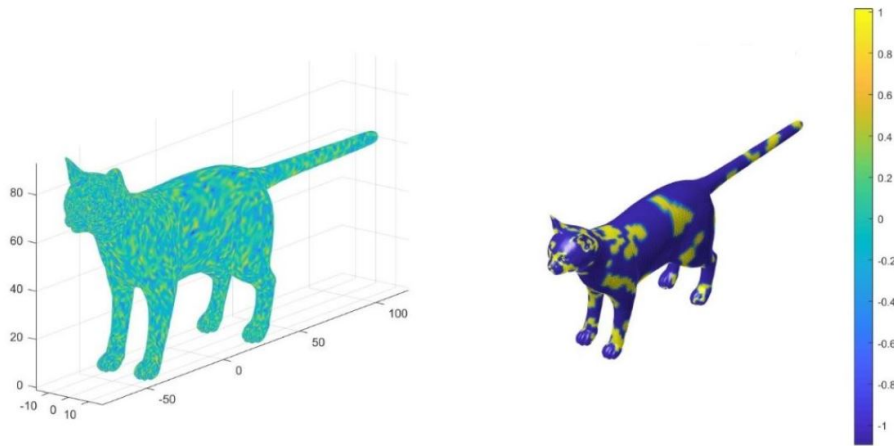


Figure 8: Left: Random initial data. Right: Spots. Reaction term. $b = -0.2$.

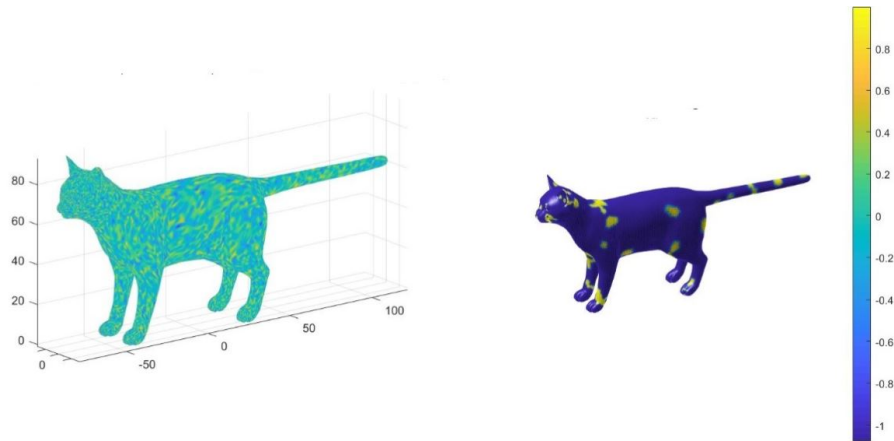


Figure 9: Left: Random initial data. Right: Spots. Reaction term. $b = -0.3$.

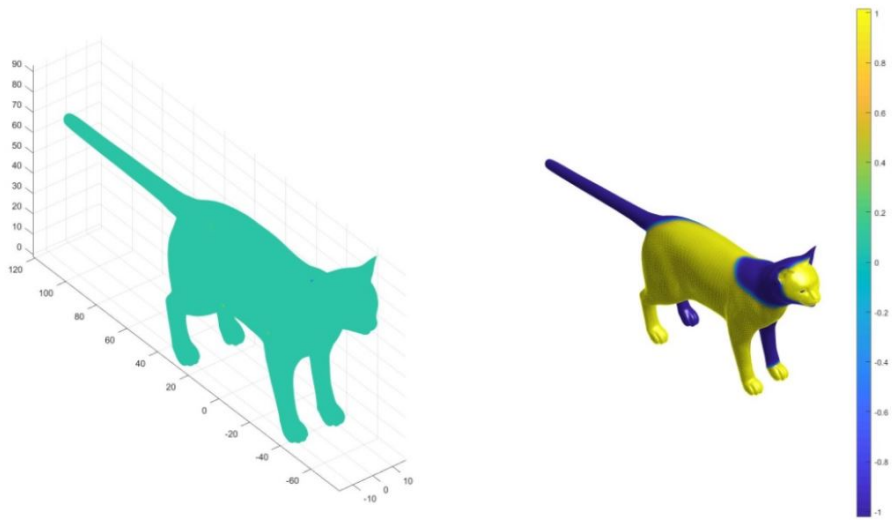


Figure 10: Left: Initial sparse random data. Right: The stripes created with Allen-Cahn model.

The example in Fig.10 illustrates the stripes created by Allen-Cahn model, given a sparse random initial data on the surface. The solution exhibits the phase separation property, see Fig.11 i.e. the solution tends to ± 1 . An interface of width ϵ is created between the two phases.

The examples in Fig.12, Fig.15 show examples of generated spots for almost invariant surfaces. Giving the same initial random data, the modified

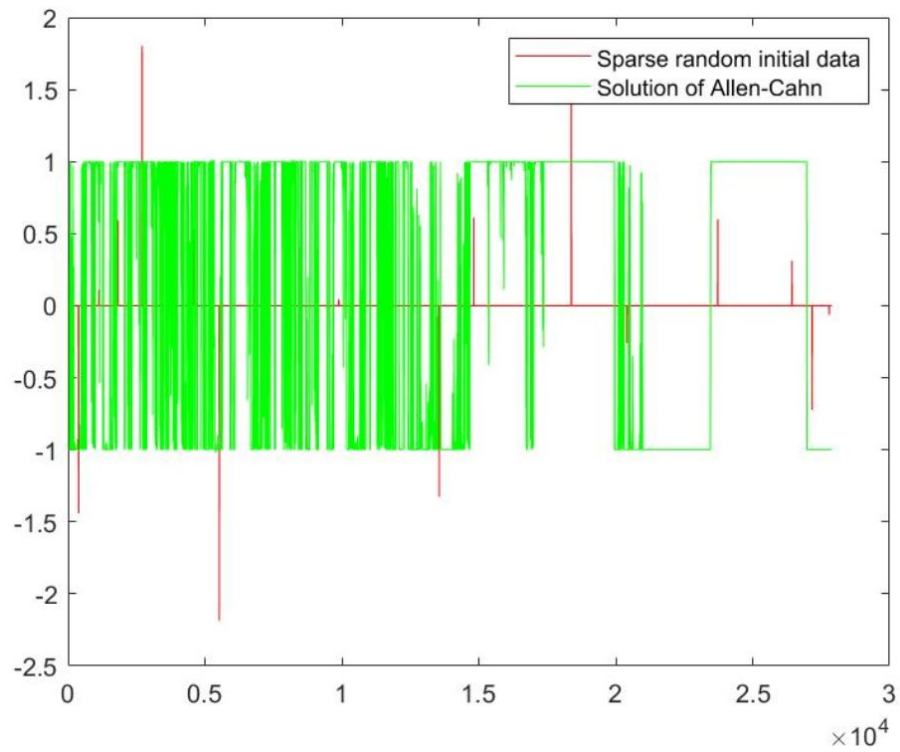


Figure 11: Graph of initial data and of numerical solution to Allen-Cahn model.

Allen-Cahn model leads to spots in the three isometric surfaces located in corresponding regions. This invariance property resides in the fact that the modified Allen-Cahn is invariant to isometries due to the Laplace-Beltrami operator which is invariant to isometries, and moreover the nonlinear part of the reaction term of the governing equation depends only on u , and not on the local coordinates on the surface.

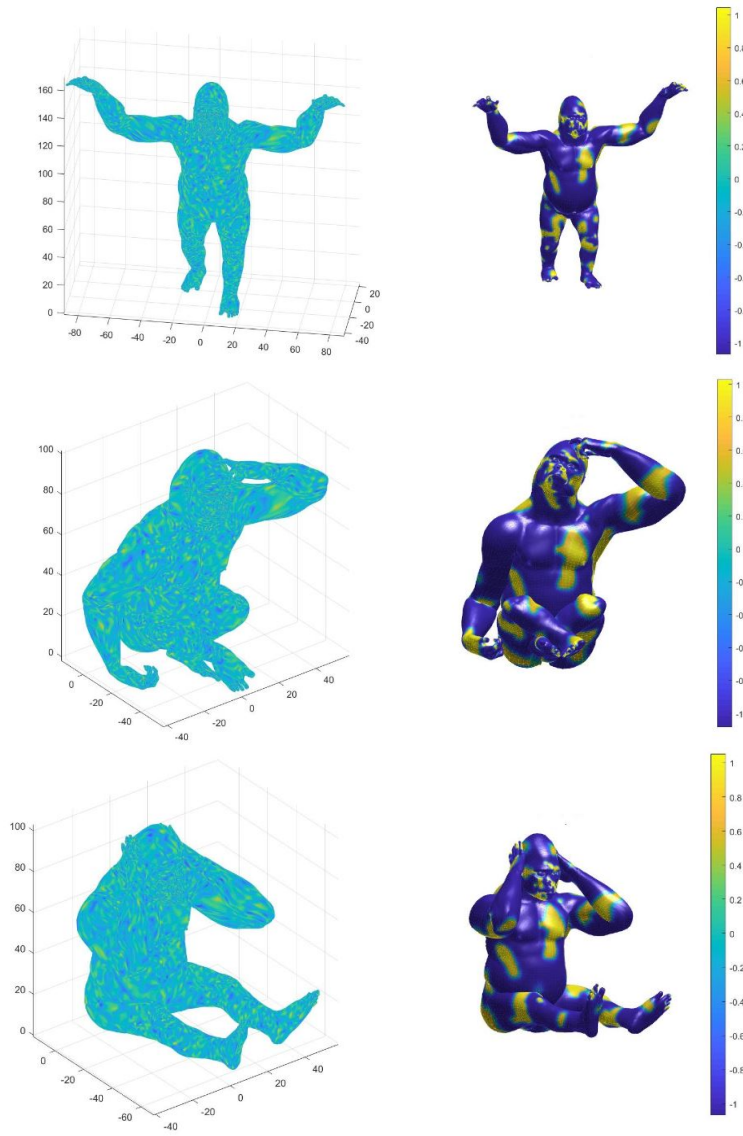


Figure 12: Various almost isometric shapes with generated global spot patterns in corresponding regions on the surfaces. Giving the same initial random data defined on surface, the modified A-Cahn model leads to spots in the three isometric surfaces located in corresponding regions.

4.2 Localized patterns with modified Allen-Cahn model

The locality of the modified model is an important property and is illustrated in examples below. While in the case of Allen-Cahn it fails see Fig. 14, this locality is satisfied only by the modified Allen-Cahn model, see Fig. 13. Given an initial data in a compact domain, by means of the modified A-Cahn model, the generated pattern will be formatted only in this domain.

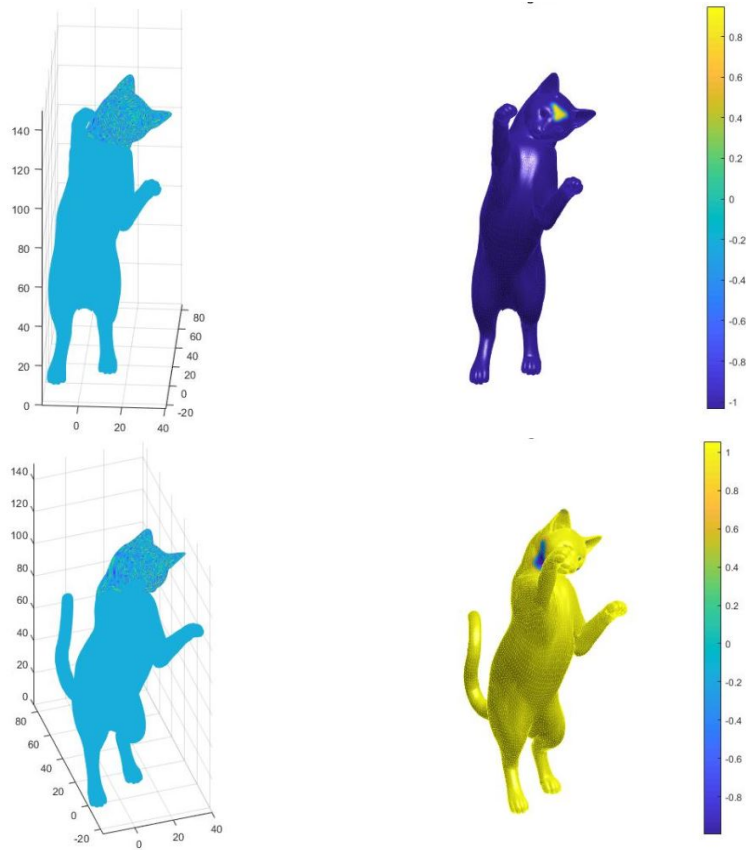


Figure 13: Left top and bottom. Localized random initial data. Top right: Generated spots remain localized, residing in the area where the initial data was defined. $b = -0.08$. 1200 iterations. $dt = 0.9$. Bottom right. Inverted spots. $b = 0.08$.

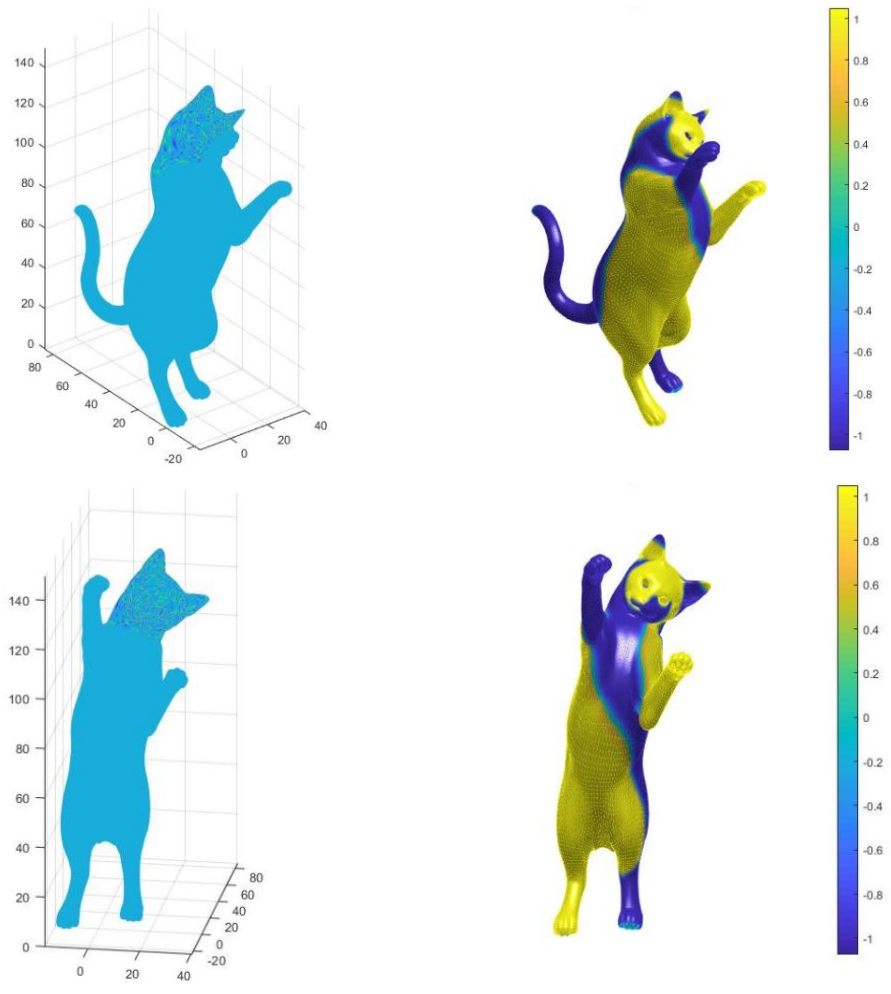


Figure 14: Left top and bottom. Localized random initial data. Right. Generated stripes (Allen-Cahn, $b = 0$), see two views on the pattern on the surface. Generated pattern is not local, moulding on the whole surface.

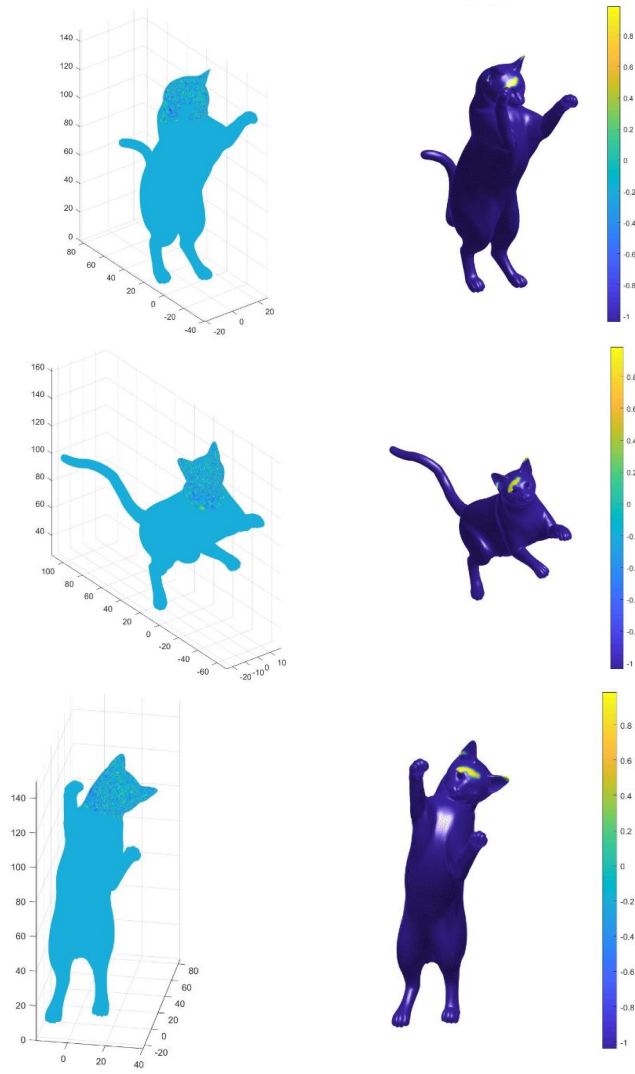


Figure 15: Various almost isometric shapes with generated local spot patterns in corresponding regions on the surfaces. Giving the same initial random data defined on compact set on the surfaces, the modified A-Cahn model leads to localized spots residing in the same compact set, in the three isometric surfaces in corresponding regions. $b = -0.08$.

5 Conclusions

We propose a slight modification of the known reaction-diffusion Allen-Cahn model on surfaces. Unlike with the Allen-Cahn model, generating only stripes, the modified model can be used to generate patterns in form of spots/inverted spots. The dependence of the kind of pattern on the new introduced reaction term is investigated. Furthermore, a simple and efficient operator based splitting scheme is employed to discretize the equation. Numerical examples show the solution of the corresponding PDE under varying initial conditions to illustrate various patterns and the underlying local or global generated patterns. In future work we will include extensions of the modified Allen-Cahn flow on deforming geometries and exploring possible applications of such patterns for shape analysis/correspondence.

References

- S.M. Allen, J.W.Cahn. A microscopic theory for antiphase boundary motion and its application to antiphase domain coarsening. *Acta Metall*, 27(6):1085–1095, 1979.
- L. Chen. Phase-field models for microstructure evolution. *Annual Review of Materials Research*, 32(2):112–140, 2002.
- M. Cheng, J.A. Warren. An efficient algorithm for solving phase field crystal model. *J. Comp. Physics*, 227(12):6241–6248, 2008.
- Y. Choukroun, G. Pai and R. Kimmel. Sparse approximation of 3d meshes using the spectral geometry of the hamiltonian operator. *Journal of Mathematical Imaging and Vision*, 60:941–952, 2018.
- S. Kondo. The reaction-diffusion system: a mechanism for autonomous pattern formation in the animal skin. *Genes Cells*, 7(6):535–541, 2011.
- C. Piret. The orthogonal gradients method: A radial basis functions method for solving partial differential equations on arbitrary surfaces. *J. Comput. Physics*, 231(14):4662–4675, 2013.
- G. Dziuk, C.M. Elliott. Surface finite elements for parabolic equations. *IMA Journal of Numerical Analysis*, 27(2):262–292, 2007.
- J. Nagumo, S. Arimoto, S. Yoshizawa. An active pulse transmission line simulating nerve axon. *Proceedings of the IRE*, 50(10):2061–2070, 1962.
- M. Kowalczyk, Y. Liu. Nondegeneracy of the saddle solution of the allen-cahn equation. *Proceedings of the American Mathematical society*, 138(12):4319–4329, 2011.